HHS Public Access

Author manuscript

Optom Vis Sci. Author manuscript; available in PMC 2016 April 01.

Published in final edited form as:

Optom Vis Sci. 2015 April ; 92(4): 437–446. doi:10.1097/OPX.0000000000000559.

Refractive Error and Ocular Parameters: Comparison of Two SD-OCT Systems

Lisa A. Ostrin, OD, PhD, FAAO, **Jill Yuzuriha, OD**, and **Christine F. Wildsoet, OD, PhD, FAAO**

University of California, Berkeley, School of Optometry, Berkeley, California (JY, CFW), and University of Houston, College of Optometry, Houston, Texas (LAO)

Abstract

Purpose—Spectral domain optical coherence tomography (SD-OCT) was used to examine the influence of refractive error (RE) on foveal retinal and choroidal thicknesses and scleral canal width (SCW). The performance of the Cirrus and Bioptigen SD-OCT instruments was compared in the same eyes.

Methods—Both eyes of forty healthy human subjects, ages 22 to 38 years, were dilated and imaged, with the Cirrus OCT, using 6 mm 5-line rasters collapsed into one line, one centered on the fovea and one bisecting the optic nerve head. Seventy-two of the same eyes were imaged with the Bioptigen OCT, using 6 mm × 6 mm scans, one centered on the fovea and one on the optic nerve head. Subfoveal retinal and choroidal thicknesses and SCW were measured. Axial lengths (AL) and REs were obtained using an IOLMaster and a Grand Seiko autorefractor, respectively.

Results—Only right eyes were included in analyses. Spherical equivalent REs ranged from −12.18 to +8.12 D (mean: −3.44 ± 4.06 D), and ALs ranged from 20.56 to 29.17 mm (mean: 24.86 ± 1.91 mm). Myopia was associated with relatively thin choroids at the fovea ($p<0.05$) but normal retinal thickness. SCW was significantly correlated with AL as measured with the Bioptigen OCT ($p<0.05$). Retinal and choroidal thicknesses recorded with the Bioptigen OCT tended to be smaller than values obtained with the Cirrus OCT (mean difference: 5.63 and 24.76 μm, respectively), while the converse was true for the SCW (mean difference: 25.45 μm).

Conclusions—The finding that high myopes tend to have a thinner subfoveal choroid is consistent with previous studies. That high myopia was linked to enlarged scleral canals may help to explain the increased risk of glaucoma in myopia. Observed differences obtained with the Cirrus and Bioptigen instruments urge caution in comparing results collected with different instruments.

Keywords

SD-OCT; myopia; retina; choroid; refractive error

Corresponding author: Lisa Ostrin, University of Houston, College of Optometry, 4901 Calhoun, Houston, TX 77204, laostrin@gmail.com.

Lisa A. Ostrin and Jill Yuzuriha contributed equally to this work and are considered co-first authors.

Presented in part at American Academy of Optometry annual meeting, November 2013, Seattle, Washington.

Refractive errors result when there is a mismatch between the optical power and the axial length of an eye. Theoretically, myopia may result from an eye being either too long or its optical components too powerful, leading to images of distant objects being formed in front of the retina. Conversely, hyperopia may result from an eye being either too short or its optical components not powerful enough, leading to equivalent images being formed behind the retina. However, most refractive errors are caused by abnormalities of ocular length, specifically of the vitreous chamber, and while both myopia and hyperopia can be optically corrected to eliminate the above focusing errors, myopia carries an increased risk of a number of sight-threatening ocular pathologies, including retinal detachment,[1] choroidal neovascularization,[2] cataracts,[3] and glaucoma.[3] Because the latter risks also increase with the amount of myopia,[4] high myopia is frequently referred to as “pathological myopia.”

The excessive elongation of the vitreous chamber that underlies most myopia may be expected to have adverse consequences for the structures making up the wall of the vitreous chamber, including the retina and choroid, unless there are mechanisms to allow these tissues to accommodate the expanded scleral surface. Such structural changes, for example, as a product of excessive growth and stretching, would offer a plausible explanation for the reported increased risk of many ocular pathologies. Reports of a thinner nerve fiber layer[5] and choroid[6, 7] in myopes are consistent with excessive stretch in these eyes. The current study sought to further investigate refractive error-related differences, with a focus on foveal retinal and choroidal changes, as well as changes in optic nerve dimensions, because of their potential to help elucidate the pathophysiology of myopia.

Advances in optical coherence tomography (OCT) now allow non-invasive high resolution cross-sectional imaging of key ocular tissues, including the retina, choroid, and nerve fiber layer.[8, 9] The ocular imaging applications of this technology were described as early as 1988,[10] and it has enjoyed a surge of usage in recent years, paralleling improvements in the technology.[11–13] Spectral domain OCT (SD-OCT), represents the latest generation of commercial ophthalmic OCT technology and makes use of spectral interferometry and a Fourier transformation to obtain cross-sectional images of various ocular structures, including the retina, in vivo. Among commercially available instruments employing this technology, some can acquire over 20,000 A-scans per second, with some offering cellular level resolution, achieved by averaging multiple B-scan images.[14]

In previously published OCT studies, the subfoveal choroid was reported to be much thinner in highly myopic eyes than in emmetropic eyes.[15, 16] The choroid, a dense vascular structure underlying the retina, plays an important role in meeting the high nutrient and energy demands of the outer retina, with the central avascular foveal region being dependent on the choroid exclusively. In high myopia, the choroid is frequently structurally compromised, with both choroidal neovascularization[16, 17] and chorioretinal atrophy[18] being reported. Previous studies have also shown correlations between axial length and some other ocular parameters, apart from central refractive error, for example, peripapillary retinal nerve fiber layer thickness.[19] However, the influence of myopia on foveal retinal thickness is of interest as it addresses the question of whether the mechanisms operating early in development to draw photoreceptors together to establish the fovea[20, 21] can be reactivated during the development of myopia to counter any stretching influences to maintain its normal

structure.[22] It is currently unclear as to what the effects of axial growth are on the cone spacing directly at the center of the fovea.[23]

Structural changes in the optic nerve head have also been reported in myopic eyes. For example, the lamina cribrosa, a porous collagenous structure providing the floor of the optic nerve cup through which retinal ganglion cell axons exit the eye to form the optic nerve, is reported to be thinner in highly myopic eyes than in non-myopic eyes.[24, 25] It is noteworthy that lamina cribrosa thinning has been associated with glaucoma, for which myopes carry an increased risk.[25, 26] The lamina cribrosa bridges the scleral canal, the width of which has also been linked to glaucomatous damage,[27, 28] with larger canals being associated with increased risk. Thus it is of interest to know whether myopic eyes also have larger than normal scleral canals.

The first objective of this study was to determine how axial length and/or refractive error influences key ocular structural parameters. Foveal retinal thickness and scleral canal width data were collected, as well as corneal curvature, anterior chamber depth and subfoveal choroidal thickness, to explore correlations, if any, between refractive errors and axial length.

The second objective was to compare data obtained using the Cirrus SD-OCT, which is now commonly used in clinical settings, and the Bioptigen SD-OCT, which thus far has been used primarily in research, with limited clinical application of its hand-held option for infant retinal imaging.[29] It is recognized that ocular tissue thickness data collected using different SD-OCT instruments, each with their own unique segmentation protocol, may not be interchangeable.[30] As advanced OCT technology becomes more widely used in patient care, it is important to quantify such differences for application in clinical decision-making. Foveal retinal thickness was selected as one of two parameters for this comparison to address the question of whether these two instruments can be used interchangeably. The second parameter was scleral canal width, a key optic nerve structural parameter. Given that SD-OCT instruments are subject to decreases in sensitivity and resolution as imaging depth increases, it was deemed important to establish whether this parameter could be measured reliably with the Cirrus and/or Bioptigen SD-OCT instruments. A past study found that the sum of the prelaminar tissue and the lamina cribrosa thickness can exceed the depth of signal penetration with standard OCT techniques.[31] While the measurement of the scleral canal width requires adequate signal strength at a depth similar to that required for lamina cribrosa thickness measurement, it is plausible that the former parameter may be measurable but not the latter, at least in some eyes, since measurement of scleral canal width involves a horizontal plane, and measurement of lamina cribrosa thickness, a vertical plane. As such data can potentially provide insights into the increased risk of glaucoma in myopes, information on the utility of these advanced SD-OCT instruments for this application is in itself of high clinical relevance.[23]

METHODS

Forty healthy subjects were recruited to participate in this study, the majority being female (32/40). The racial composition of study subjects included 32 Asians and 8 Caucasians.

Subjects included staff and students at the University of California, Berkeley School of Optometry, as well as family and friends of lab members. Inclusion criteria included an age range of 18–40 years and best corrected visual acuity of 20/20 or better. Exclusion criteria included ocular pathology or disease, prior ocular surgery or ocular trauma. Informed consent was obtained in accordance with the Declaration of Helsinki and institutionally approved human subjects protocols.

Subjects first underwent screening tests to determine their suitability for the study. Each subject was asked to complete a brief history form, including information about personal and family ocular history. Both eyes of each subject were then measured (total of 80 eyes). Monocular distance visual acuities with current refractive corrections were measured to verify best-corrected visual acuities. Refractive errors were determined with an open field autorefractor (Grand Seiko, Co. ltd, Japan) while the subject viewed a distant letter chart, and spherical equivalent values derived for each eye. Ocular parameters, including axial length (AL), corneal curvature, anterior chamber depth, and white-to-white (corneal) diameter were measured using the IOLMaster (Carl Zeiss Meditec, Inc., Dublin, CA). An anterior segment slit lamp examination was performed and intraocular pressure (IOP) measured using Goldmann applanation tonometry to confirm the subject's suitability for pupil dilation and rule out high pressure. Eyes were then dilated with tropicamide (1.0%) and phenylephrine (2.5%) in preparation for OCT imaging.

Once dilation was complete, both eyes of each of 40 subjects were imaged using the Cirrus SD-OCT. The Cirrus OCT system utilizes a light source of 840nm with 27,000 scans per second, and is capable of 5 μm axial and 15 μm transverse resolution. The sequence of Cirrus OCT scans included a high definition 6 mm 5-line raster (collapsed into one line) centered over the fovea, a second scan passing through the fovea and optic nerve head, and a 200 × 200 optic disc cube scan centered over the optic nerve head. Only scans with signal strengths of 6 or greater were used in analyses.

Sixty eyes of a subset of 30 subjects were also imaged using the Bioptigen SD-OCT. Images were acquired while the instrument was mounted, as opposed to handheld, with the chinrest in place. The Bioptigen OCT scans acquired from each eye included one 6 mm × 6 mm rectangular scan centered on the fovea, and one centered on the optic nerve head. Scans consisted of 1000 a-scans per b scan, with three frames per scan, registered and averaged. The Bioptigen OCT system uses an 840 nm engine with 93nm bandwidth internal source providing < 3 μm tissue resolution and with > 32,000 lines per second acquisition and display.

OCT scans were collected in the upright, rather than converted, configuration, then analyzed using the built-in calipers for each instrument. Macular scans were first evaluated to determine whether the posterior surface of the subfoveal choroid could be resolved. When image resolution allowed, both total retinal and choroidal thicknesses at the fovea were measured. Retinal thickness (RT) was measured at the center of the foveal pit, vertically from the inner surface of the inner limiting membrane to the inner surface of the hyper-reflective band representing the retinal pigment epithelial (RPE) layer. The thickness of the immediately adjacent choroid (CT) was measured axially from the posterior surface of the

RPE to the anterior surface of the hyper-reflective area demarcating choroid-sclera interface. The latter interface was resolvable in 60 of 72 eyes.

For optic nerve head scans, the scleral canal width (SCW) was measured as the widest horizontal dimension of the canal opening, demarcated by the scleral boundary. In order to account for changes in scan length based on each subject's axial length and optical components, a lateral magnification factor was determined for each eye. Lateral, or transverse, magnification for each eye was determined using a 4-surface model eye; values for corneal thickness and posterior radius of curvature, lens thickness and radii of curvatures, and indices of refraction for the cornea, aqueous, lens and vitreous were taken from Gullstrand's schematic eye, as described by Li, et al.[23] Each eye's measured AL, average corneal radius of curvature and anterior chamber depth were incorporated into the model to scale its scleral canal width data.

Although both eyes of all subjects were measured, statistical analyses reported here are limited to right eyes only because of the expected high correlation between the two eyes of individual subjects. Paired t-tests were applied to refraction and biometric data collected with the IOLMaster to verify the latter. For subsequent analyses, only right eye data were used. Correlations between AL and refractive error, as well as other biometric parameters and structural parameters extracted from the OCT images, were assessed. Paired t-tests and Bland-Altman analyses were used to assess agreement between the two instruments. For all analyses, statistical significance was defined as $p<0.05$.

RESULTS

Subjects were 22 to 38 years old (mean: 25.44 ± 3.04 years), and spanned a large range of refractive errors. Table 1 summarizes the refractive error and biometric data for both right and left eyes. No significant differences were found between them, for any of the parameters listed.

Of the 40 right eyes included in subsequent analyses, refractive errors spanned a wide range (equivalent spherical refractive error (SRE): range: −12.18 to +8.12 D; mean: −3.44 ± 4.06 D), with 29 classified as myopic (SRE ≤ −0.75 D), 9 classified as emmetropic (SRE: −0.75 to +0.75 D), and 2 classified as hyperopic (SRE ≥ +0.75 D). The profile for the subset of 30 eyes imaged with both the Cirrus and the Bioptigen OCT instruments was similar with the exclusion of the hyperopes. They were myopic on average but included emmetropes (mean: −4.15 ± 3.29 D; range −12.18 to +0.57 D, see Table 1).

As with refractive errors, ALs also spanned a broad range, from 20.56 to 29.17 mm (mean: 24.9 ± 1.91 mm). There was a significant linear relationship between AL and SRE, with the more myopic eyes exhibiting longer ALs ($p<0.0005$, Figure 1A, Table 2). Anterior chamber depths ranged from 2.77 to 4.15 mm (mean: 3.63 ± 0.29 mm), and also exhibited significant linear correlations with both AL and SRE ($p<0.005$, Figure 1B), reflecting the deeper anterior chambers of more myopic eyes. Corneal curvature ranged from 40.87 to 46.76 D (mean: 43.94 ± 1.44 D), with longer eyes having flatter corneas (Figure 1C). Longer eyes also have larger corneas, expressed in terms of white-to-white diameter (WWD), which

ranged from 10.9 to 13.1 mm (mean: 12.2 ± 0.45 mm; Figure 1D). Both corneal curvature and WWD were significantly correlated with AL ($p<0.05$). All eyes had IOPs within normal limits (mean IOP: 14.48 ± 2.73 mmHg; range 8 to 20 mmHg).

Foveal retinal thickness (RT) data were obtained with both the Cirrus and Bioptigen OCT instruments for 30 eyes. Sample scans from each instrument are shown in Figure 2, and data extracted from scans are summarized in Table 3. Mean values for RT at the foveal pit were 198.23 ± 17.12 μm (range: 164 to 244 μm) for the Cirrus OCT and 193.97 ± 18.19 μm (range: 161 to 237 μm, Figure 3a) for the Bioptigen OCT. While the foveal RT data derived from Cirrus OCT and Bioptigen appear quite similar, these two sets of data were significantly different statistically (paired t-test, $p<0.05$), and a follow-up Bland-Altman analysis revealed a trend towards higher values for the Cirrus OCT compared to the Bioptigen OCT (Figure 3e), with an average difference of 5.63 μm. General trends toward increasing thickness with increasing myopia are also suggested by both sets of data but proved not to be statistically significant for either instrument (Cirrus OCT: $r^2=0.02$, $p=0.45$; Bioptigen OCT: $r^2=0.05$, $p=0.21$). However, a statistically significant linear correlation between foveal RT, as measured with the Bioptigen OCT, and AL was observed ($r^2=0.13$, $p=0.03$).

Subfoveal choroidal thickness (CT) data are available for 21 eyes (70%) of the 30 eyes imaged with both the Cirrus and Bioptigen OCTs, reflecting insufficient image quality for the remaining 9 eyes. Hyperopic eyes are not represented in these 21 eyes, which ranged in SRE from −12.18 to +0.57 D, with a mean of −4.15 ± 3.29 D. Here again, there was a significant difference between values obtained with the Cirrus and Bioptigen OCTs ($p<0.005$); mean values were 219.48 ± 65.11 μm (range: 116 to 416 μm) and 194.71 ± 75.38 μm (range: 109 to 415 μm) respectively. Data for individual eyes are shown plotted against each other in Figure 3d. Bland-Altman analysis again suggests a trend towards higher CT for the Cirrus OCT compared to the Bioptigen OCT (24.76 μm average difference; Figure 3f). CT data, plotted against AL in Figure 3b for both instruments, show a trend towards decreasing thickness with increasing myopia, opposite in direction to that described above for foveal RT. Statistically, there was a significant linear correlation between SRE and subfoveal CT for both instruments (Cirrus: $r^2=0.34$, $p<0.05$; Bioptigen OCT: $r^2=0.32$, $p<0.05$). Additionally, there was a significant linear correlation between AL and subfoveal CT for both instruments (Cirrus: $r^2=0.50$, $p<0.05$; Bioptigen OCT: $r^2=0.40$, $p<0.05$)

Scleral canal width (SCW) data are available for 28 of the 30 imaged eyes; the Bioptigen OCT images from one subject contained too much shadow to allow the scleral canal to be delineated, and the rim of the scleral canal was also not sufficiently well visualized in one of the Cirrus OCT images to allow measurement. Raw data were scaled using calculated lateral magnification factors, which ranged from 0.77 to 1.26 (Table 3). Values extracted from Cirrus and Bioptogen OCT images ranged from 998 to 1945 μm (mean: 1365.29 ± 227.16 μm) and 1025 to 1986 μm (mean: 1382.17 ± 205.73 μm) respectively (Figure 4a). Values for individual eyes, obtained with the two instruments, are shown plotted against each other in Figure 4b. While there is no statistically significant difference between the two data sets ($p=0.06$), results of Bland-Altman analysis suggest that, on average, values obtained with the Bioptigen OCT are larger, by 25.4 ± 68.1 μm, than those obtained with the Cirrus OCT

(Figure 4c). Corrected SCWs, plotted against SRE (Figure 5a), show a trend towards increasing canal size with increasing myopia, with this relationship being statistically significant for the Bioptigen OCT (r^2=0.13, p<0.05) but not the Cirrus OCT (r^2=0.05, p=0.23). Here again, the corrected SCW increased significantly with AL for the Bioptigen OCT (r^2=0.19, p<0.05) but not the Cirrus OCT (r^2=0.11, p=0.08).

DISCUSSION

With increasing axial length, we found that foveal RT increases, subfoveal CT decreases, and the SCW increases. Differences between the two OCT instruments used, the Bioptigen OCT and Cirrus OCT, were small but significant, with the Cirrus OCT yielding greater values in the axial direction and the Bioptigen yielding greater values in the lateral direction. Two of the above mentioned parameters, RT and SCW, exhibited significant linear correlations with axial length, albeit only when measured with the Bioptigen OCT.

The observed association of myopia with increased axial length, as well as the relationships between SRE and other ocular parameters (corneal curvature, anterior chamber depth, and white-to-white corneal diameter), are consistent with previous findings in other studies.[32–34] The consistent finding that myopes have longer eyes predicts that these patients will be at greater risk of complications associated with stretching of posterior ocular tissues, such as retinal detachments and posterior staphylomas, and justifies increased monitoring to allow early detection of sight-threatening changes.

Previous studies have found an association between myopia and an increased risk for glaucoma.[35, 36] Our analyses revealed statistically significant correlations between both SRE and axial length with SCW, measured with the Bioptigen OCT. However, SRE only accounted for 7–9% of the variance in SCW, suggesting that other factors must also be contributing to the increased risk of glaucoma in myopes. Given this finding, we undertook a secondary analysis to examine the correlation between SRE and intraocular pressure; however, these parameters were not significantly correlated. Of other factors besides intraocular pressure that may contribute to the increased risk of glaucoma in myopic eyes, one could be the thickness of the lamina cribrosa, which provides support for nerve fibers entering the optic nerve. However in the current study, the lamina cribrosa was not clearly delineated in most of the images collected, from both Cirrus and Bioptigen OCT instruments, and thus lamina cribrosa thickness data are not available for our study population. Nonetheless, it is likely that such measurements will be possible in the near future, with further improvements in SD-OCT technology, with the potential to provide additional insights into the relationship between myopia and glaucoma.

The observation that foveal RT (measured at the trough of the foveal pit) tends to increase with increasing myopia in our study (although not significantly so), is consistent with previous reports,[18, 37, 38] and is particularly interesting, given that the latter studies also described thinning of the peripheral retina in myopic eyes. Together these data suggest that the central retina is somehow protected against the stretching forces accompanying increased globe expansion, and assumed to underlie the peripheral retinal thinning in myopic eyes.[38] Note that this is not the case for the central (subfoveal) choroid, which showed

relative thinning with increasing myopia, as also reported in other studies.[39] The CT changes are consistent with passive stretching, a product of increased globe expansion, and are significant because the choroid represents the exclusive source of oxygen and nutrients to the central foveal region and a critical source of the same for the outer retina more generally. While these myopia-related choroidal changes might be expected to carry an increased risk of adverse ocular complications, it is of interest that recent studies have suggested that increased axial length might be protective against diabetic retinopathy and macular edema, for which myopic eyes carry reduced risks.[40, 41] A reduction in metabolic demands due to the overall thinning of the retina, a product of the increase in axial length, has been offered as one possible explanation for these protective effects, implying that a thinner than normal choroid may not present a problem. However, further investigations are warranted to fully understand the mechanism underlying the apparent protection of high myopia against the above retinal complications.

In this study, both eyes of each subject were imaged. Previous studies have shown a statistically significant correlation between right and left eyes of the same subjects as measured with OCT.[42, 43] Therefore, right eyes only were randomly chosen to be included in the analyses. While the subjects in the current study represented a wide range of SREs, especially on the myopic end of the spectrum, it should also be noted that the study population was relatively homogeneous, being mostly female, at the younger end of age spectrum (18 to 40 years), mostly Asian American and biased towards myopia. The number of subjects was also relatively small. Previous studies suggest that ethnic and gender differences exist in macular retinal thickness and optic nerve head parameters. Significant differences in macular structure have been reported in normal Asian and Caucasian populations.[44] In addition, it has been reported that women have thinner macular retinal thickness[45] and choroidal thickness.[46] A larger study of similar design encompassing wider demographics would allow the results to be more generalizable. In particular, increased representation of hyperopes would be highly instructive in understanding whether observed structural changes in myopic eyes are specific to their refractive errors, and/or a product of increased axial lengths.

The second goal of this study was to compare measurements obtained with two different instruments, the Cirrus and Bioptigen OCT devices. Despite the advanced OCT technology incorporated into the Cirrus and Bioptigen instruments, the posterior choroidal surface could be delineated in only 70% of subjects' images, precluding extraction of CT data for the remaining subjects. Emmetropic and hyperopic eyes proved most problematic, as well as those with heavily pigmented ocular structures, which limited penetration and thus resolution. Further improvements in imaging techniques to allow measurement of CT in these eyes should be made a research priority. Nonetheless, our success rate in obtaining CT data was similar to that of Manjanuth and colleagues who were able to reliably measured CT with the Cirrus SD-OCT in only 74% of their subjects.[47] Although not employed here, other studies have inverted the OCT image in order to increase depth penetration. Inversion of images obtained with the Bioptigen OCT was found to increase image contrast and resolution of the posterior choroidal surface as compared to the upright version.[48] The same study found upright images from the Cirrus OCT were superior to upright images collected with the Bioptigen OCT. The required improvement in resolution for such ocular structures

would seem achievable with further advances in imaging, perhaps involving a longer wavelength of light and/or a modified “enhanced depth imaging” technique.

Previous studies have been undertaken to compare the repeatability and reproducibility of subfoveal choroidal measurements with various OCT instruments.[9, 49] In one study, two separate measurements of choroidal thickness were performed on 43 subjects using three OCT instruments, including the Cirrus OCT. With the Cirrus OCT an intraclass correlation coefficient (ICC) of 0.958 (0.919–0.978) was found.[9] Similarly, Benavente-Pérez A imaged the choroid with SD-OCT (SOCT Copernicus) in 11 subjects on two separate occasions and reported an ICC of 0.99.[49] Although in the current study only one image was measured from each subject, SD-OCT imaging of the subfoveal choroid has been shown to be repeatable and reproducible.[9, 49]

The values for retinal and choroidal thicknesses measured with the Cirrus and Bioptigen OCT instruments proved significantly different statistically, although these differences may not be clinically relevant. For example, differences in retinal thicknesses obtained with the Bioptigen and Cirrus OCTs represented an average difference of only 2.4%. The fact that values for foveal RTs and subfoveal CTs collected with the Bioptigen OCT tended to be smaller than those collected with the Cirrus OCT, might reflect variations in scaling related to the optics of eyes with different axial lengths. However, these parameters are both axial in nature and the opposite trend was observed in SCW data, with slightly larger values being recorded with the Bioptigen OCT than with the Cirrus OCT. These differences between the two instruments cannot be attributed to the delineation software differences as noted in previous studies, given that a single author (JY) manually analyzed all images, applying the same delineation criteria to images from both instruments. Two previous studies comparing the Cirrus SD-OCT instrument to other commercially available OCT instruments also found significant instrument-related differences in extracted retinal and nerve fiber layer thickness data,[50, 51] although the Bioptigen SD-OCT was not included in these studies. Further research quantifying differences between results with the Bioptigen OCT and other instruments currently in clinical use will be needed if the former is to gain clinical utility in the future.

This study was limited by poor resolution of some images. For example, excessive shadowing in one subject's images made it impossible to delineate the margins of the scleral canal. The lack of an internal fixation target in the Bioptigen OCT, as present in the Cirrus OCT, also makes imaging with the former instrument more difficult for subjects with poor fixation ability. Nonetheless, resolution limited the visibility of the lamina cribrosa for both instruments, precluding related thickness measurements.

A strength of the current study is that all images were processed by one experimenter, applying the same criteria for delineating structures to all images, while a potential limitation is that time of day at which the measurements were taken was not standardized, given that a number of ocular parameters, including choroidal thicknesses are subject to diurnal fluctuation.[52] However, we do not expect our failure to control for this variable to have led to spurious trends, but rather it would have increased the noise in our data, perhaps explaining the failure of some trends not to reach statistical significance.

In summary, results of the current study confirmed refractive error-related differences in central retinal and choroidal thickness previously reported by others as well as differences in scleral canal width. As the number of people with myopia continues to grow worldwide, quantifying such differences and understanding their functional implications ranks high in terms of clinical significance, because early diagnosis of sight-threatening conditions is critical to sight preservation. Finally, with advances in imaging technology for examining such critical ocular structures, it is imperative that comparative studies, such as the one described here, are undertaken to allow meaningful comparison of data collected with different instrumentation.

ACKNOWLEDGMENTS

NIH NEI K08 EY022696 to LO, NIH NEI T35 to JY, NIH NEI P30 EY07551 to University of Houston College of Optometry, Dr. Julia Benoit for statistical support.

REFERENCES

1. Tornquist R, Stenkula S, Tornquist P. Retinal detachment. A study of a population-based patient material in Sweden 1971–1981. I. Epidemiology. Acta Ophthalmol (Copenh). 1987; 65:213–222. [PubMed: 3604613]
2. Hotchkiss ML, Fine SL. Pathologic myopia and choroidal neovascularization. Am J Ophthalmol. 1981; 91:177–183. [PubMed: 6162388]
3. Pan CW, Cheung CY, Aung T, Cheung CM, Zheng YF, Wu RY, Mitchell P, Lavanya R, Baskaran M, Wang JJ, Wong TY, Saw SM. Differential associations of myopia with major age-related eye diseases: the Singapore Indian Eye Study. Ophthalmology. 2013; 120:284–291. [PubMed: 23084122]
4. Flitcroft DI. The complex interactions of retinal, optical and environmental factors in myopia aetiology. Prog Retin Eye Res. 2012; 31:622–660. [PubMed: 22772022]
5. Zhao L, Wang Y, Chen CX, Xu L, Jonas JB. Retinal nerve fibre layer thickness measured by Spectralis spectral-domain optical coherence tomography: The Beijing Eye Study. Acta Ophthalmol. 2014; 92:e35–e41. [PubMed: 23981513]
6. Ho M, Liu DT, Chan VC, Lam DS. Choroidal thickness measurement in myopic eyes by enhanced depth optical coherence tomography. Ophthalmology. 2013; 120:1909–1914. [PubMed: 23683921]
7. Vincent SJ, Collins MJ, Read SA, Carney LG. Retinal and choroidal thickness in myopic anisometropia. Invest Ophthalmol Vis Sci. 2013; 54:2445–2456. [PubMed: 23482471]
8. Keane PA, Sadda SR. Imaging chorioretinal vascular disease. Eye (Lond). 2010; 24:422–427. [PubMed: 20010789]
9. Yamashita T, Yamashita T, Shirasawa M, Arimura N, Terasaki H, Sakamoto T. Repeatability and reproducibility of subfoveal choroidal thickness in normal eyes of Japanese using different SD-OCT devices. Invest Ophthalmol Vis Sci. 2012; 53:1102–1107. [PubMed: 22247474]
10. Fercher AF, Mengedoht K, Werner W. Eye-length measurement by interferometry with partially coherent light. Opt Lett. 1988; 13:186–188. [PubMed: 19742022]
11. Lim LS, Cheung G, Lee SY. Comparison of spectral domain and swept-source optical coherence tomography in pathological myopia. Eye (Lond). 2014; 28:488–491. [PubMed: 24434661]
12. Al-Haddad C, Antonios R, Tamim H, Noureddin B. Interocular symmetry in retinal and optic nerve parameters in children as measured by spectral domain optical coherence tomography. Br J Ophthalmol. 2014; 98:502–506. [PubMed: 24393664]
13. Leung CK. Diagnosing glaucoma progression with optical coherence tomography. Curr Opin Ophthalmol. 2014; 25:104–111. [PubMed: 24370973]
14. Kiernan DF, Mieler WF, Hariprasad SM. Spectral-domain optical coherence tomography: a comparison of modern high-resolution retinal imaging systems. Am J Ophthalmol. 2010; 149:18–31. [PubMed: 20103039]

15. Fujiwara T, Imamura Y, Margolis R, Slakter JS, Spaide RF. Enhanced depth imaging optical coherence tomography of the choroid in highly myopic eyes. Am J Ophthalmol. 2009; 148:445–450. [PubMed: 19541286]
16. Ikuno Y, Tano Y. Retinal and choroidal biometry in highly myopic eyes with spectral-domain optical coherence tomography. Invest Ophthalmol Vis Sci. 2009; 50:3876–3880. [PubMed: 19279309]
17. Shimada N, Ohno-Matsui K, Yoshida T, Futagami S, Tokoro T, Mochizuki M. Development of macular hole and macular retinoschisis in eyes with myopic choroidal neovascularization. Am J Ophthalmol. 2008; 145:155–161. [PubMed: 17988641]
18. Ohsugi H, Ikuno Y, Oshima K, Tabuchi H. 3-D choroidal thickness maps from EDI-OCT in highly myopic eyes. Optom Vis Sci. 2013; 90:599–606. [PubMed: 23604298]
19. Park SH, Park KH, Kim JM, Choi CY. Relation between axial length and ocular parameters. Ophthalmologica. 2010; 224:188–193. [PubMed: 19864929]
20. Hendrickson A, Possin D, Vajzovic L, Toth CA. Histologic development of the human fovea from midgestation to maturity. Am J Ophthalmol. 2012; 154:767–778. e2. [PubMed: 22935600]
21. Vajzovic L, Hendrickson AE, O'Connell RV, Clark LA, Tran-Viet D, Possin D, Chiu SJ, Farsiu S, Toth CA. Maturation of the human fovea: correlation of spectral-domain optical coherence tomography findings with histology. Am J Ophthalmol. 2012; 154:779–789. e2. [PubMed: 22898189]
22. Dubis AM, McAllister JT, Carroll J. Reconstructing foveal pit morphology from optical coherence tomography imaging. Br J Ophthalmol. 2009; 93:1223–1227. [PubMed: 19474001]
23. Li KY, Tiruveedhula P, Roorda A. Intersubject variability of foveal cone photoreceptor density in relation to eye length. Invest Ophthalmol Vis Sci. 2010; 51:6858–6867. [PubMed: 20688730]
24. Jonas JB, Xu L. Histological changes of high axial myopia. Eye (Lond). 2014; 28:113–117. [PubMed: 24113300]
25. Jonas JB, Berenshtein E, Holbach L. Lamina cribrosa thickness and spatial relationships between intraocular space and cerebrospinal fluid space in highly myopic eyes. Invest Ophthalmol Vis Sci. 2004; 45:2660–2665. [PubMed: 15277489]
26. Park HY, Jeon SH, Park CK. Enhanced depth imaging detects lamina cribrosa thickness differences in normal tension glaucoma and primary open-angle glaucoma. Ophthalmology. 2012; 119:10–20. [PubMed: 22015382]
27. Sigal IA, Yang H, Roberts MD, Burgoyne CF, Downs JC. IOP-induced lamina cribrosa displacement and scleral canal expansion: an analysis of factor interactions using parameterized eye-specific models. Invest Ophthalmol Vis Sci. 2011; 52:1896–1907. [PubMed: 20881292]
28. Norman RE, Flanagan JG, Rausch SM, Sigal IA, Tertinegg I, Eilaghi A, Portnoy S, Sled JG, Ethier CR. Dimensions of the human sclera: Thickness measurement and regional changes with axial length. Exp Eye Res. 2010; 90:277–284. [PubMed: 19900442]
29. Muni RH, Kohly RP, Sohn EH, Lee TC. Hand-held spectral domain optical coherence tomography finding in shaken-baby syndrome. Retina. 2010; 30:S45–S50. [PubMed: 20386092]
30. Wolf-Schnurrbusch UE, Ceklic L, Brinkmann CK, Iliev ME, Frey M, Rothenbuehler SP, Enzmann V, Wolf S. Macular thickness measurements in healthy eyes using six different optical coherence tomography instruments. Invest Ophthalmol Vis Sci. 2009; 50:3432–3437. [PubMed: 19234346]
31. Lee EJ, Kim TW, Weinreb RN, Park KH, Kim SH, Kim DM. Visualization of the lamina cribrosa using enhanced depth imaging spectral-domain optical coherence tomography. Am J Ophthalmol. 2011; 152:87–95. e1. [PubMed: 21570046]
32. Alfonso JF, Ferrer-Blasco T, Gonzalez-Meijome JM, Garcia-Manjarres M, Peixoto-de-Matos SC, Montes-Mico R. Pupil size, white-to-white corneal diameter, and anterior chamber depth in patients with myopia. J Refract Surg. 2010; 26:891–898. [PubMed: 20027985]
33. Goss DA, Cox VD, Herrin-Lawson GA, Nielsen ED, Dolton WA. Refractive error, axial length, and height as a function of age in young myopes. Optom Vis Sci. 1990; 67:332–338. [PubMed: 2367086]
34. Logan NS, Davies LN, Mallen EA, Gilmartin B. Ametropia and ocular biometry in a U.K. university student population. Optom Vis Sci. 2005; 82:261–266. [PubMed: 15829853]

35. Mitchell P, Hourihan F, Sandbach J, Wang JJ. The relationship between glaucoma and myopia: the Blue Mountains Eye Study. Ophthalmology. 1999; 106:2010–2015. [PubMed: 10519600]
36. Xu L, Wang Y, Wang S, Wang Y, Jonas JB. High myopia and glaucoma susceptibility the Beijing Eye Study. Ophthalmology. 2007; 114:216–220. [PubMed: 17123613]
37. Park S, Kim SH, Park TK, Ohn YH. Evaluation of structural and functional changes in non-pathologic myopic fundus using multifocal electroretinogram and optical coherence tomography. Doc Ophthalmol. 2013; 126:199–210. [PubMed: 23471724]
38. Lam DS, Leung KS, Mohamed S, Chan WM, Palanivelu MS, Cheung CY, Li EY, Lai RY, Leung CK. Regional variations in the relationship between macular thickness measurements and myopia. Invest Ophthalmol Vis Sci. 2007; 48:376–382. [PubMed: 17197557]
39. Nishida Y, Fujiwara T, Imamura Y, Lima LH, Kurosaka D, Spaide RF. Choroidal thickness and visual acuity in highly myopic eyes. Retina. 2012; 32:1229–1236. [PubMed: 22466466]
40. Man RE, Sasongko MB, Sanmugasundram S, Nicolaou T, Jing X, Wang JJ, Wong TY, Lamoureux EL. Longer axial length is protective of diabetic retinopathy and macular edema. Ophthalmology. 2012; 119:1754–1759. [PubMed: 22627119]
41. Rand LI, Krolewski AS, Aiello LM, Warram JH, Baker RS, Maki T. Multiple factors in the prediction of risk of proliferative diabetic retinopathy. N Engl J Med. 1985; 313:1433–1438. [PubMed: 3864010]
42. Kelty PJ, Payne JF, Trivedi RH, Kelty J, Bowie EM, Burger BM. Macular thickness assessment in healthy eyes based on ethnicity using Stratus OCT optical coherence tomography. Invest Ophthalmol Vis Sci. 2008; 49:2668–2672. [PubMed: 18515595]
43. Spaide RF, Koizumi H, Pozzoni MC. Enhanced depth imaging spectral-domain optical coherence tomography. Am J Ophthalmol. 2008; 146:496–500. [PubMed: 18639219]
44. Pilat AV, Proudlock FA, Mohammad S, Gottlob I. Normal macular structure measured with optical coherence tomography across ethnicity. Br J Ophthalmol. 2014; 98:941–945. [PubMed: 24518076]
45. Harb E, Hyman L, Fazzari M, Gwiazda J, Marsh-Tootle W, Group CS. Factors associated with macular thickness in the COMET myopic cohort. Optom Vis Sci. 2012; 89:620–631. [PubMed: 22525127]
46. Ooto S, Hangai M, Yoshimura N. Effects of sex and age on the normal retinal and choroidal structures on optical coherence tomography. Curr Eye Res. 2015; 40:213–225. [PubMed: 25153829]
47. Manjunath V, Taha M, Fujimoto JG, Duker JS. Choroidal thickness in normal eyes measured using Cirrus HD optical coherence tomography. Am J Ophthalmol. 2010; 150:325–329. e1. [PubMed: 20591395]
48. Lin P, Mettu PS, Pomerleau DL, Chiu SJ, Maldonado R, Stinnett S, Toth CA, Farsiu S, Mruthyunjaya P. Image inversion spectral-domain optical coherence tomography optimizes choroidal thickness and detail through improved contrast. Invest Ophthalmol Vis Sci. 2012; 53:1874–1882. [PubMed: 22410550]
49. Benavente-Perez A, Hosking SL, Logan NS, Bansal D. Reproducibility-repeatability of choroidal thickness calculation using optical coherence tomography. Optom Vis Sci. 2010; 87:867–872. [PubMed: 20818280]
50. Pierro L, Gagliardi M, Iuliano L, Ambrosi A, Bandello F. Retinal nerve fiber layer thickness reproducibility using seven different OCT instruments. Invest Ophthalmol Vis Sci. 2012; 53:5912–5920. [PubMed: 22871835]
51. Huang J, Liu X, Wu Z, Guo X, Xu H, Dustin L, Sadda S. Macular and retinal nerve fiber layer thickness measurements in normal eyes with the Stratus OCT, the Cirrus HD-OCT, and the Topcon 3D OCT-1000. J Glaucoma. 2011; 20:118–125. [PubMed: 20436366]
52. Nickla DL. Ocular diurnal rhythms and eye growth regulation: where we are 50 years after Lauber. Exp Eye Res. 2013; 114:25–34. [PubMed: 23298452]

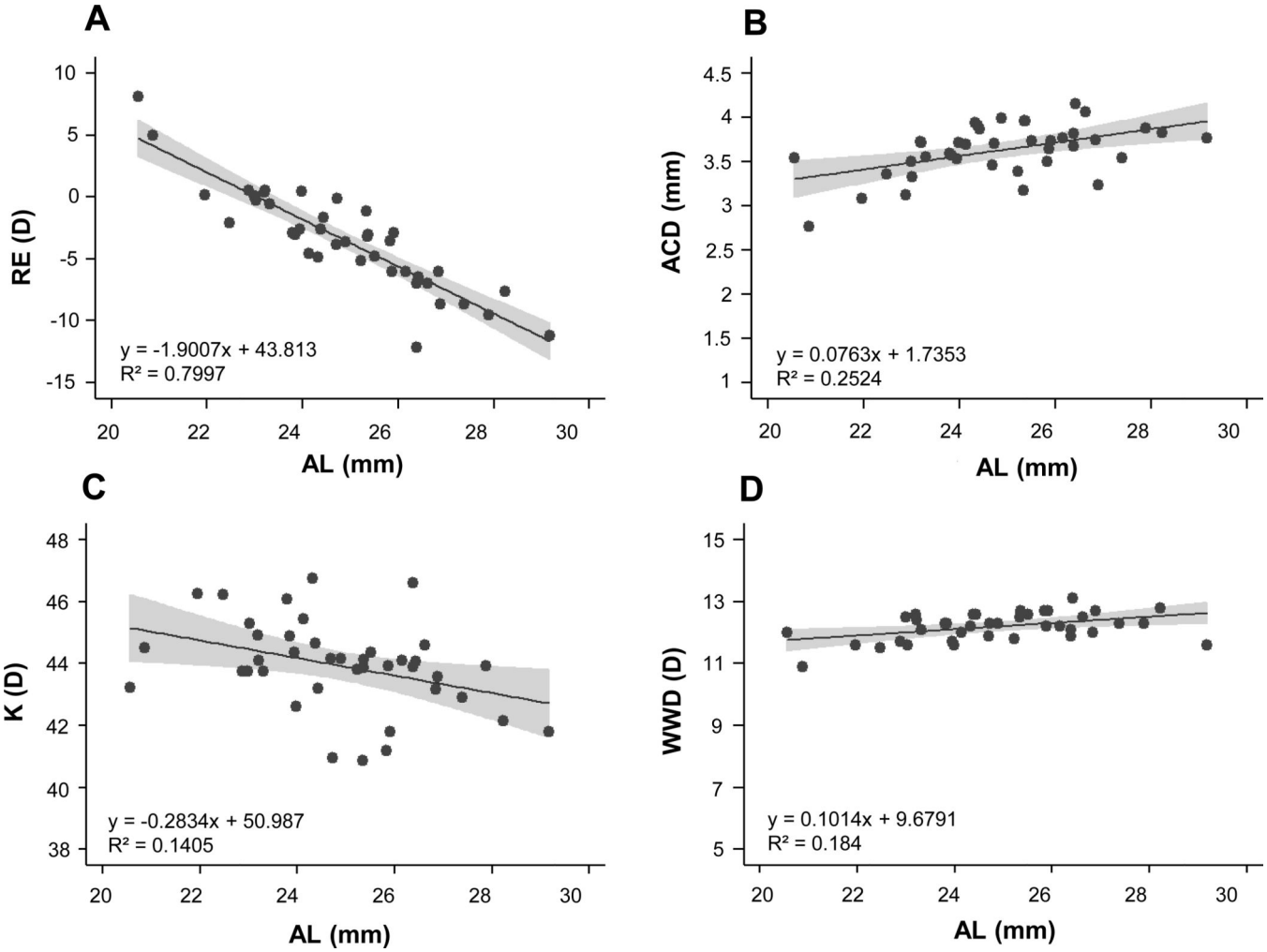

Figure 1.

Plots of **(A)** spherical equivalent refractive error (RE), **(B)** anterior chamber depth (ACD), **(C)** average corneal curvature (K) and **(D)** white-to-white corneal diameter (WWD), against axial length (AL) for right eyes only; results of regression analyses added as inserts. Shaded areas represent the 95% confidence intervals.

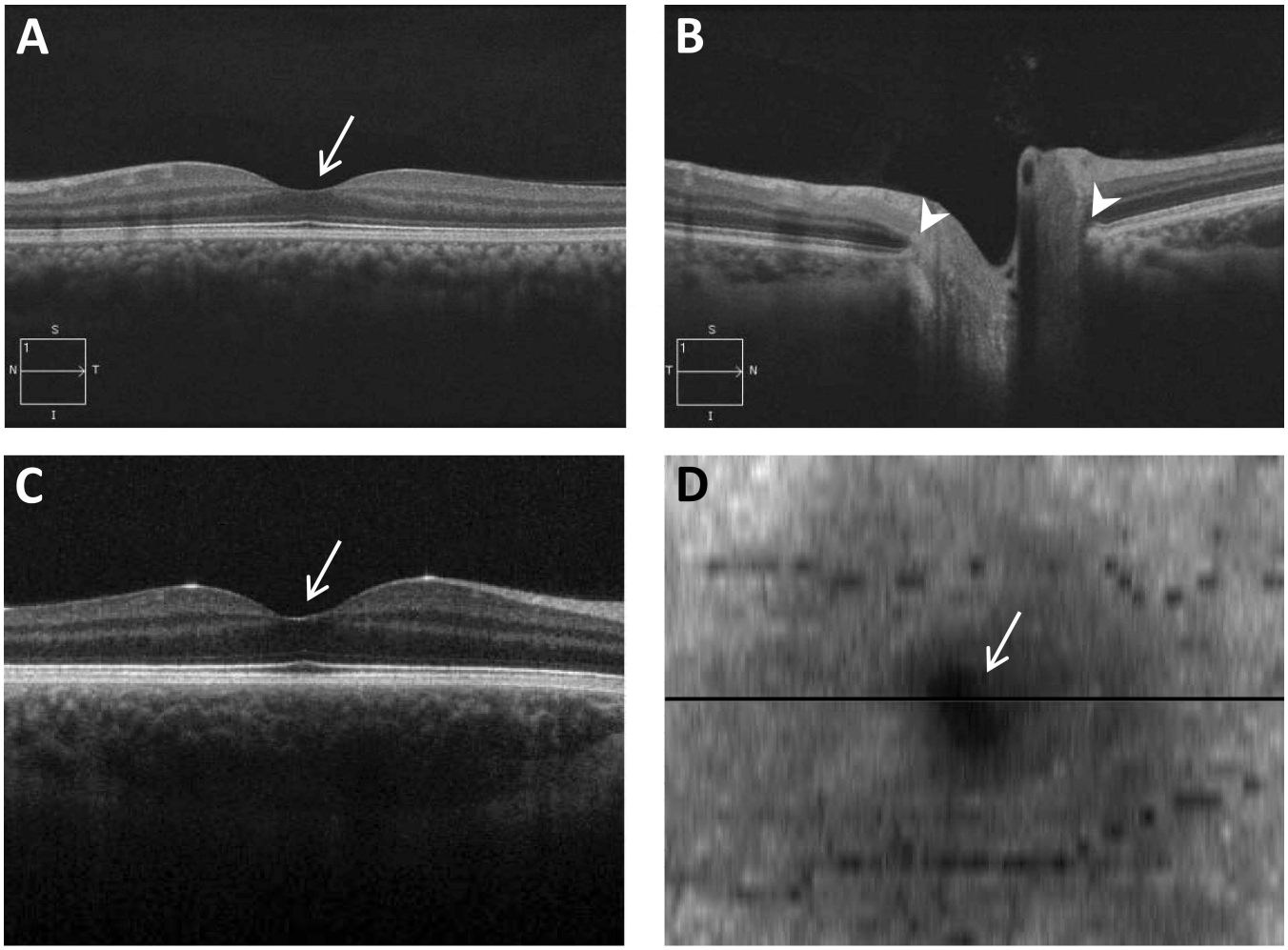

Figure 2.

Horizontal line scans (6 mm) captured using a Cirrus OCT of **(A)** the central retinal (foveal) region, and **(B)** optic nerve from one subject; C) a 6×6 mm rectangular cube scan from the Bioptigen OCT spanning the foveal region and D) corresponding en face image from another subject. Horizontal line in D shows the location of the scan in C. arrows: fovea; arrowheads: borders of scleral canal.

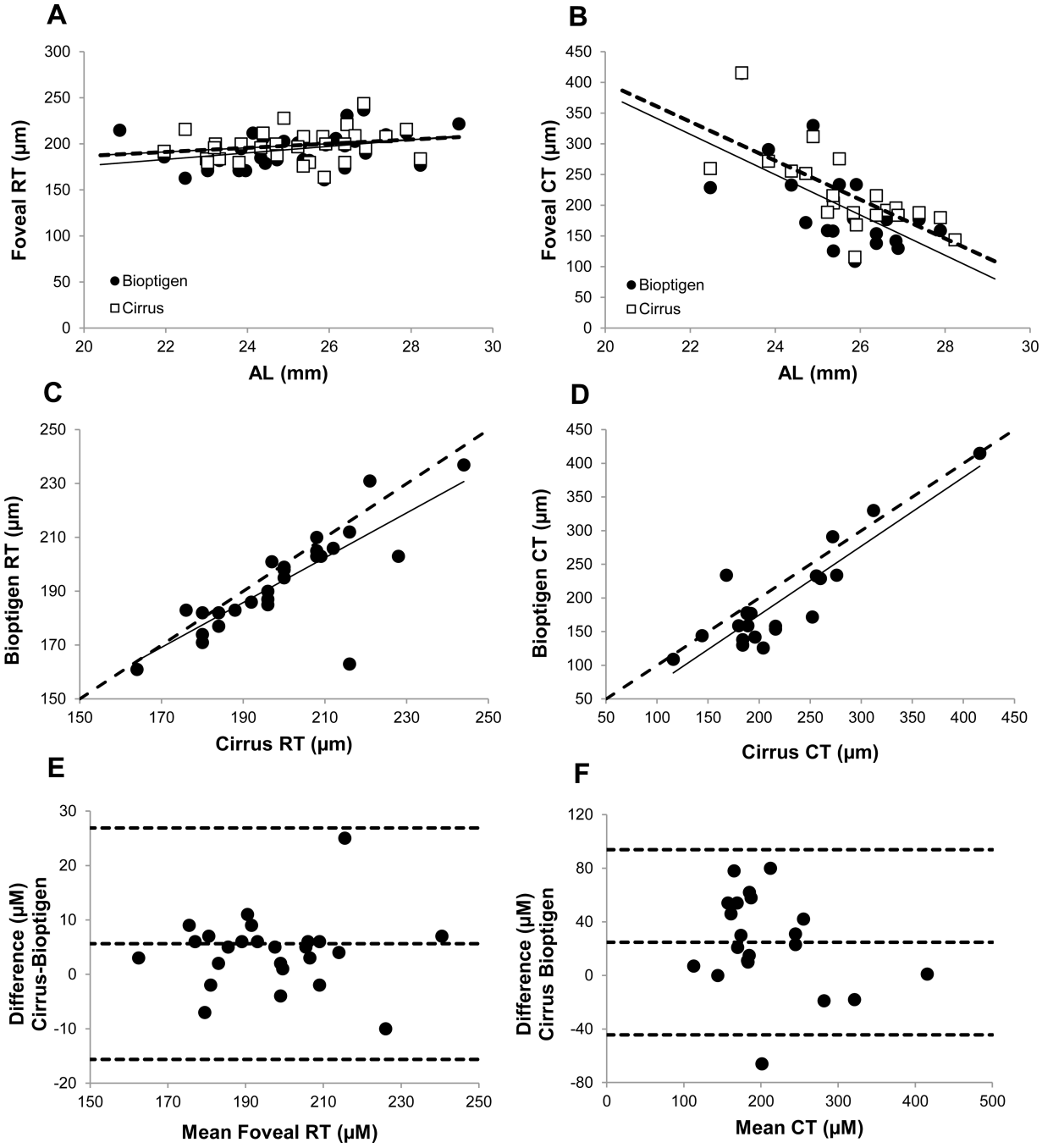

Figure 3.

Foveal retinal thickness (RT) **(A)** and subfoveal choroidal thickness (CT) **(B)** plotted against axial length (AL) for the Cirrus OCT (open squares, dashed line) and Bioptigen OCT (filled circles, solid line); RT **(C)** and CT **(D)** for Cirrus OCT plotted against equivalent data from Bioptigen OCT; dashed line is 1:1; Bland Altman analysis of differences in RT **(E)** and CT **(F)** recorded with Cirrus and Bioptigen OCTs (dashed lines are mean ± 1.96*standard deviation)

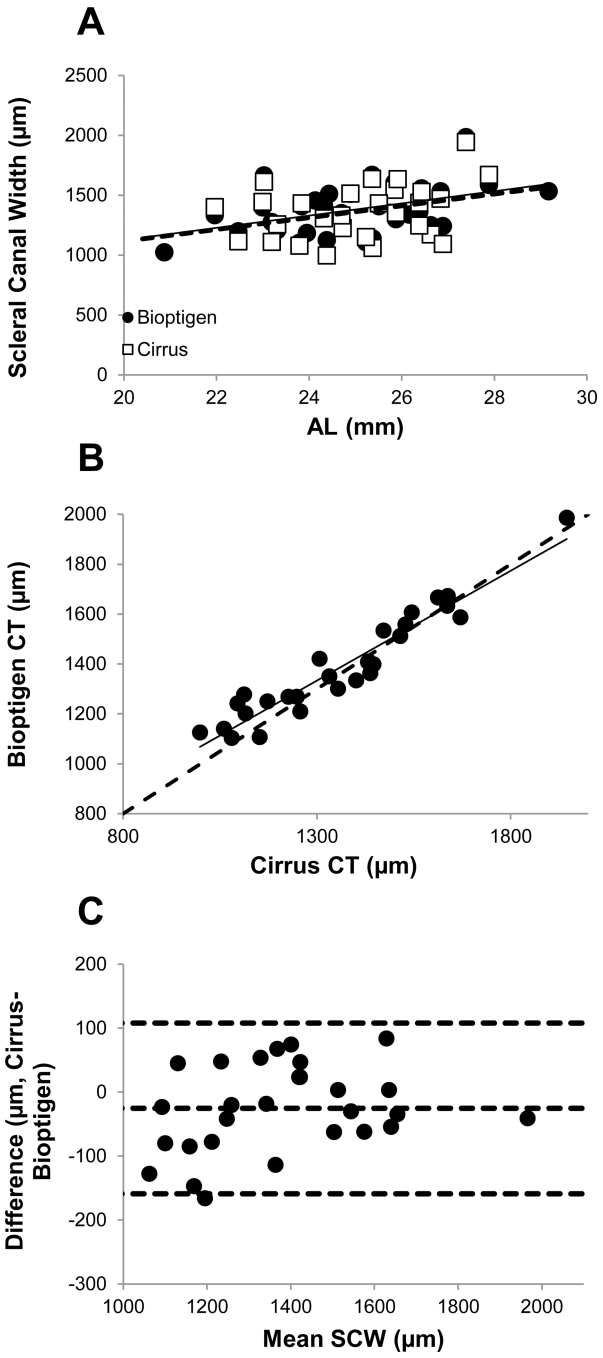

Figure 4.

(A) Scleral canal widths (SCWs) corrected for lateral magnification, plotted against axial length (AL), for both the Cirrus OCT (open squares, dashed line) and Bioptigen OCT (filled circles, solid line); **(B)** SCW measured with Cirrus OCT plotted against equivalent data from Bioptigen OCT; dashed line is 1:1; **(C)** Bland Altman analysis of differences in corrected SCW recorded with Cirrus and Bioptigen OCTs (dashed lines are mean ± 1.96*standard deviation).

Table 1

Refractive error and ocular biometric profiles of right (OD) and left (OS) eyes for 40 subjects. Right eye data for the subset of 30 patients imaged with both the Cirrus OCT and Bioptigen OCT shown in parentheses.

Parameter	Eye	Mean ± SD	Range
Spherical equivalent refractive error (SRE; D)	OD	−3.44 ± 4.06	−12.18 to +8.12
	OS	−3.48 ± 4.05	−10.81 to +7.62
	OD	(−4.09 ± 3.0)	(−9.5 to +0.57)
Axial length (AL; mm)	OD	24.86 ± 1.91	20.56 to 29.17
	OS	24.83 ± 1.89	20.4 to 28.86
	OD	(25.14 ± 1.69)	(21.96 to 28.23)
Anterior chamber depth (ACD; mm)	OD	3.63 ± 0.29	2.77 to 4.15
	OS	3.68 ± 0.27	2.87 to 4.24
	OD	(3.69 ± 0.27)	(3.08 to 4.15)
Intraocular pressure (IOP; mmHg)	OD	14.48 ± 2.73	8 to 20
	OS	14.08 ± 2.44	10 to 20
	OD	(13.72 ± 2.59)	(8 to 20)

Table 2

Linear relationship, coefficient of determination (r^2) and p value for spherical refractive error (SRE) and axial length (AL) with biometric parameters: anterior chamber depth (ACD), corneal (K) power, white-to-white diameter (WWD), intraocular pressure (IOP);

Ocular Parameters	Linear relationship	r^2 values	P values
SRE and AL	y = −0.42x + 23.41	0.80	<0.0005 *
SRE and ACD	y = −0.031x + 3.52	0.19	<0.0005 *
SRE and K power	y = −0.0092x + 43.91	0.0007	0.87
SRE and WWD	y = −0.031x + 12.09	0.077	0.08
SRE and IOP	y = 0.013x + 14.52	0.0004	0.90
AL and ACD	y = 0.076x + 1.74	0.25	<0.005 *
AL and K power	y = −0.28x + 50.99	0.14	<0.05 *
AL and WWD	y = 0.10x + 9.68	0.18	<0.05 *
AL and IOP	y = −0.21x + 19.800	0.023	0.36

* = significant relationship with $p < 0.05$.

Table 3

Foveal retinal thickness, subfoveal choroidal thickness and raw and corrected scleral canal width measured with the Cirrus OCT and Bioptigen OCT.

Ocular Parameter	Cirrus OCT	Bioptigen OCT	P value
Foveal retinal thickness (μm)	198.23 ± 17.12 (range: 164 – 244)	193.97 ± 18.19 (range: 161 – 237)	<0.05 *
Subfoveal choroidal thickness (μm)	261.27 ± 87.34 (range: 116 – 416)	220.73 ± 89.15 (range: 109 – 437)	<0.05 *
Raw scleral canal width (μm)	1318.00 ± 209.91 (range: 952 – 1728)	1338.15 ± 183.00 (range: 1053 – 1786)	=0.06
Corrected scleral canal width (μm)	1365.29 ± 227.16 (range: 998 – 1945)	1382.17 ± 205.73 (mean: 1025 – 1986)	=0.06

* = significant difference between instruments ($p < 0.05$).